

John Howard and Sawyer Baar

ME 453

23 March 2018

GFR Aluminum Wheel DIC Report

1. Introduction:

For this project we will be examining one half of an aluminum two piece wheel used by the OSU Formula SAE club, Global Formula Racing. Recently, the team started developing a carbon fiber wheel based on the aluminum wheels design. It is suspected that our current carbon fiber wheel is over engineered and stronger than the aluminum wheel. However, no testing has been performed on the aluminum wheel in order to compare against the carbon fiber design.

The goal of this project will be to examine strains and deflections of the aluminum wheel under load using full field strain information obtained through digital image correlation (DIC). This data can then be used as a reference for future wheel testing. DIC will be critical in analyzing the wheel due to the irregular geometry and various stress concentrations associated with the geometry.

For this test, the wheel will be mounted to a fixture using the 12 bolt holes. A load will then be applied to the surface where the tire bead mounts to the wheel.

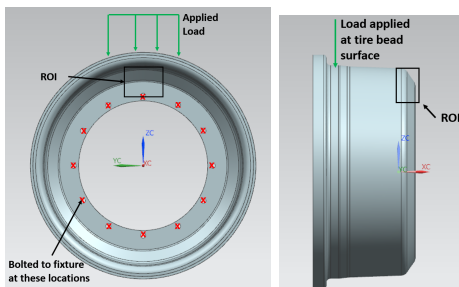


Figure 2. Loads and constraints

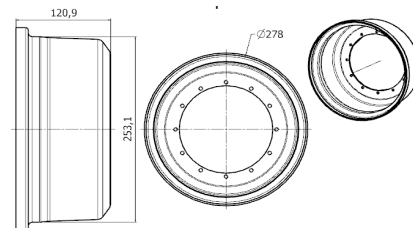


Figure 1. Wheel dimensions (units in millimeters).

The main areas of interest for digital image correlation is the area near the bolt surface and wall because of the stress concentrations at the two radii.

The aluminum wheel is made from 6061-T6, and the relevant ASTM standard for testing is *B557M-15: Standard Test Methods for Tension Testing Wrought and Cast Aluminum- and Magnesium-Alloy Products (Metric)*. This standard covers the tension testing of cast aluminum alloys, among other things, and is derived from the standard for tension testing of all metallic materials. The M designates that this is the metric standard, and will be used since GFR is a global organization and uses SI units.

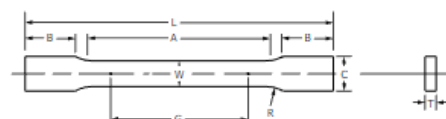


Figure 3: Dimensions of the Rectangular Tension Test specimen¹

¹ ASTM B557M-15 Fig 6.

The dimensions for the test sample will be taken straight from the ASTM B557M-15 standard. The standard states, “*6.1.1 Test specimens shall be of the full section of the material whenever practical. Otherwise, machined specimens of rectangular or round cross section shall be used.*”

We have opted to machine the test specimen from generic aluminum 6061 bar stock on a mill in the OSU Machine Shop to the correct dimensions shown in figure 3. Proper machining practices will be followed to ensure that the results are accurate and stress concentrations are minimized. This will give us an approximation of the material properties for the material.

The goal is to measure strains around the radii near the mounting surface and to measure deflections at this location, as well as at the wall of the wheel. The camera will be facing the outside edge of the wheel and the direction of the camera will be axial to the wheel. This data will also be compared to a finite element analysis using the same loading and boundary conditions in Abaqus.

2. Expected Results:

Finite element analysis was used to develop a model and predict the strains and deflections in the wheel from the loading. An exact model of the wheel tested was not used in the analysis due to a design change made last year and an original model could not be found. Unfortunately this design change affected the radii we were interested in viewing on the actual wheel. While this may cause an issue with our predicted vs actual results, the FEA model should still provide an idea of how strain will develop in the wheel. A distributed pressure load of 4.5 kN was applied to the upper rim and the model was constrained from movement or rotation at each bolt hole to simulate the current test fixtures loading and constraints. The model utilized C3D20R elements and a mesh convergence analysis was performed by examining nodes in the area shown in figure 4. Unfortunately the coordinate system used in the FEA model did not exactly match the system found in the DIC data, however it still provides decent estimates of expected values. In this case, the FEA Y axis matches closest with the DIC X axis, and the FEA X axis with the DIC Z axis. Although not perfect, for the purposes of this project the results will be presented with respect to the DIC coordinate system.

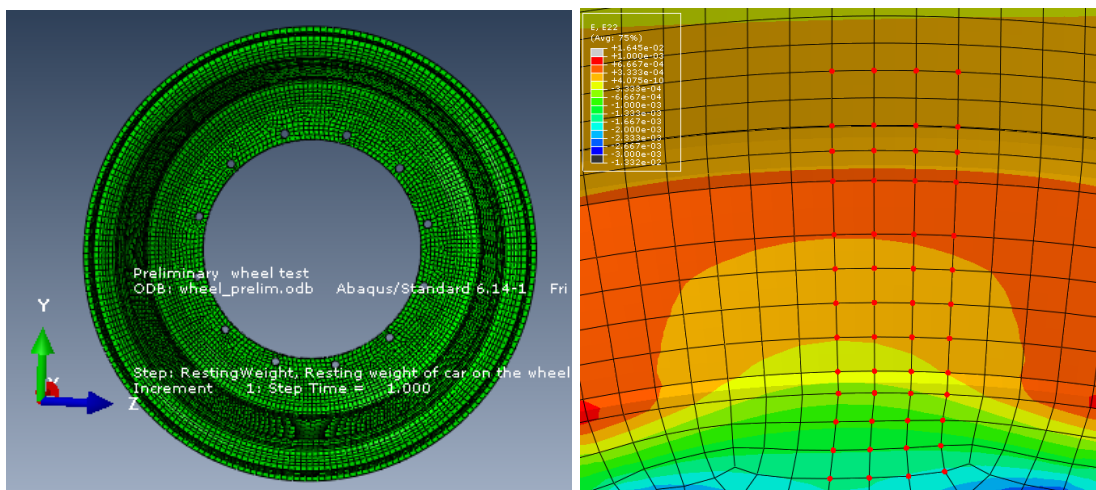


Figure 4. (Left) Wheel with FEA CSYS, (right) contour plot of E_{xx} with nodes shown

Predicted Results From FEA			
	Max	Min	Mean
X-Displacement [mm]	-0.04	-0.76	-0.24
Z-Displacement [mm]	1.18	0.26	0.78
Exx	4.43E-4	-1.74E-3	-2.10E-4
Max Principal Strain	8.59E-4	9.76E-5	4.88E-4



The aluminum wheel is made from 6061-T6 aluminum alloy. We tested a tensile sample of this same material using an Instron to determine elastic properties. From researching material properties of this aluminum alloy we were expecting a modulus of elasticity of 68.9 GPa^[1].

Figure 5. Tensile sample used for testing

3. Results:

This section details the results found from both the DIC test and the tensile sample test. The tensile test was used to determine material properties of the aluminum used in the wheel, specifically the elastic modulus. This was performed by placing the tensile in the grips of the Instron and manually loading the sample in steps while taking note of the extension at each load.



Figure 6. Tensile test setup

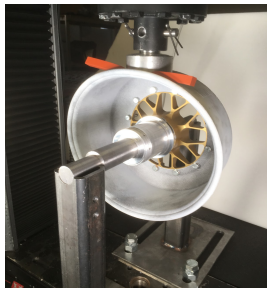


Figure 7. DIC test setup

For the DIC testing, the wheel was placed in the fixture and loaded as shown in figure 7. The load was applied in 500 N steps from 0-7000 N with pictures taken at each step. However, the results in this section only detail from 0-4500 N partially due to issues with the loading device, and partially because 4500 N is more representative of loads experienced by the formula car.

As mentioned previously, the area of the wheel being focused on was around the bolting surface and where the radius where the bolt surface flows into the barrel of the wheel. This allowed for viewing the stress concentration of the radius and a small section of the wall, which was expected to see the significant deflection.

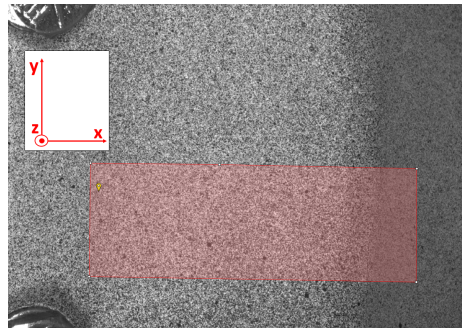


Figure 8. Image from camera and AOI used for analysis

A. Tensile Test Results

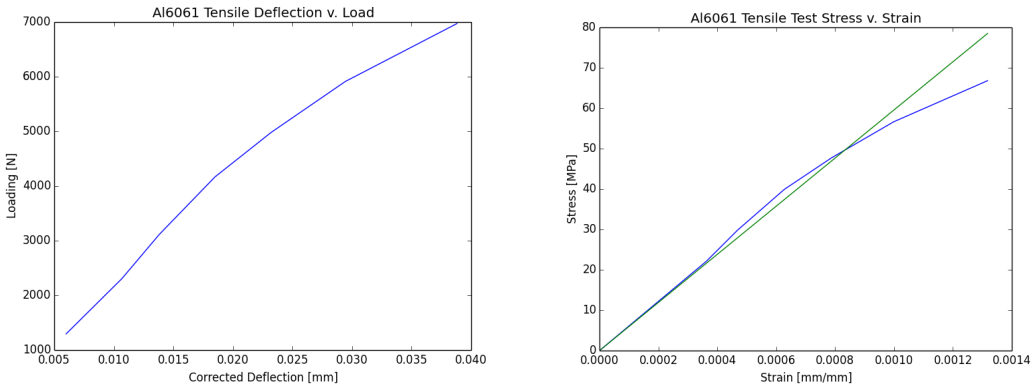


Figure 9: (Left) Load vs. Deflection and (right) Stress vs. Strain

Tensile Test Elastic Modulus Results [GPa]		
Max	Min	Average
63.6	50.7	59.6

B. Digital Image Correlation Test Results

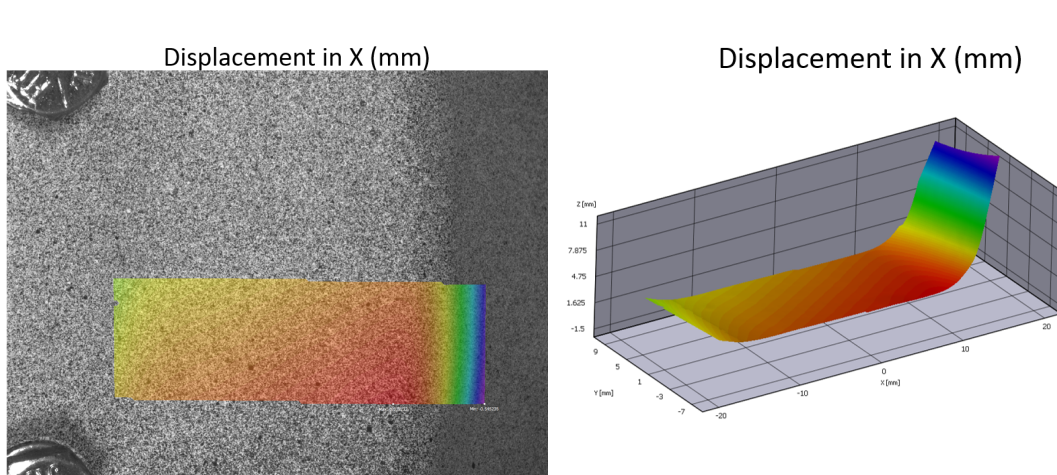


Figure 10. 2D and 3D plots of X displacement at 4.5 kN load

X Displacement (mm)	
Max	0.339
Min	-0.545
Average	0.189
Standard Deviation	0.150

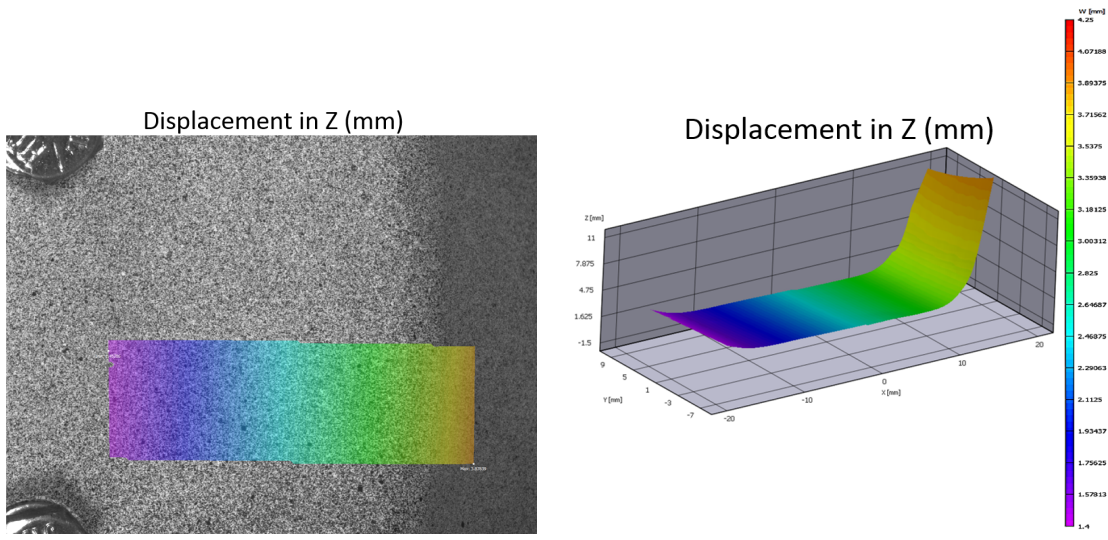


Figure 11. 2D and 3D plots of Z displacement at 4.5 kN load

Z Displacement (mm)	
Max	3.878
Min	1.458
Average	2.603
Standard Deviation	0.693

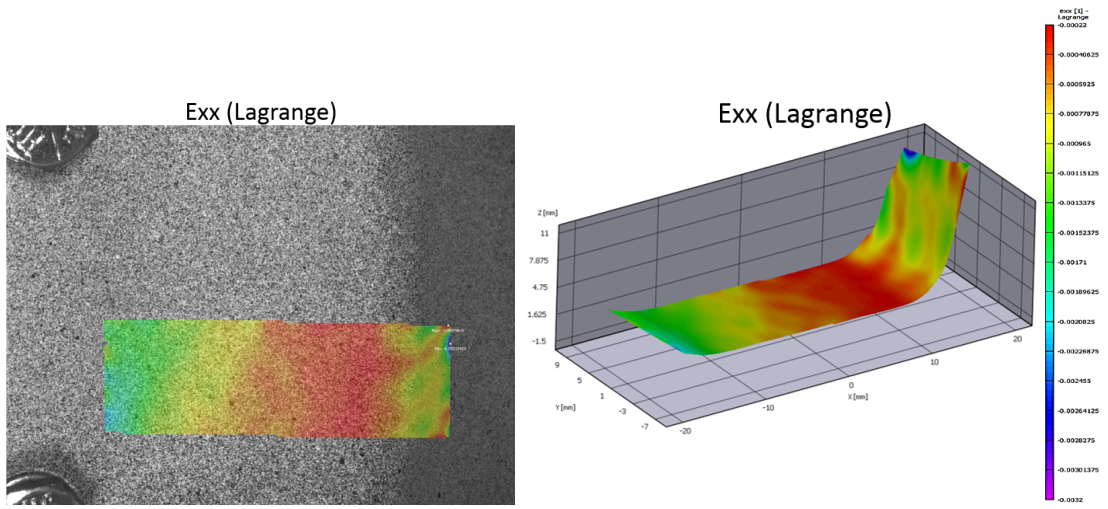


Figure 12. 2D and 3D plots of strain in the X-direction at 4.5 kN load

Exx (Lagrange)	
Max	-1.590E-5
Min	-3.104E-3
Average	-8.102E-4
Standard Deviation	4.426E-4

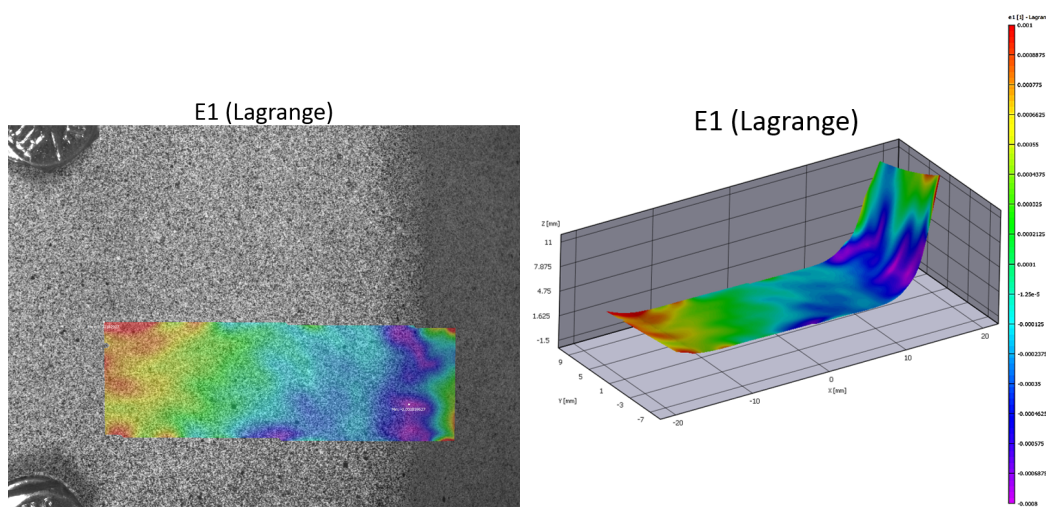


Figure 13. 2D and 3D plots of max principal strain at 4.5 kN load

E1 (Lagrange)	
Max	1.829E-3
Min	-8.596E-4
Average	6.108E-5
Standard Deviation	4.398E-4

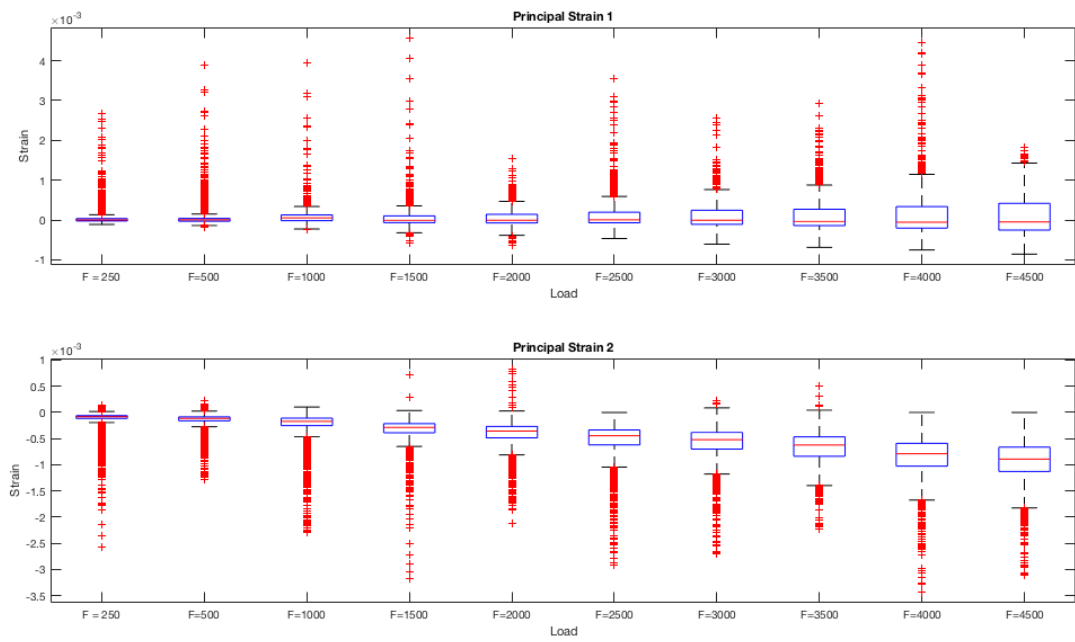


Figure 14: Distribution of principal strains in area of interest

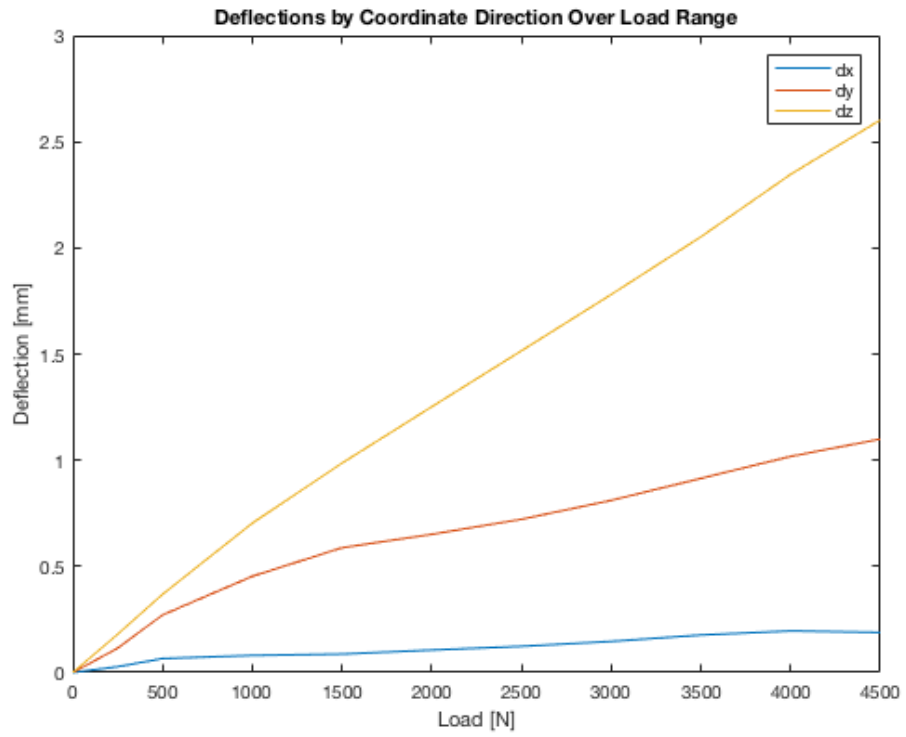


Figure 15: Average Coordinate Deflections from 0 to 4.5 kN

4. Discussion:

First, examining our tensile test, there is a noticeable discrepancy between our measured elastic modulus and the predicted value. Our measured value of 59.6 GPa is 13.5% lower than the predicted value, which could be due to the method of testing. An extensometer was not attached to the sample so extension was measured by the change in the Instron's position.

Next, the results of the DIC test provided some very interesting data. The displacements did not match well between the predicted and measured. The z-displacement was predicted to average 0.78 mm, but it averaged 2.60 mm. The x-displacement was predicted to have a minimum of -0.55 mm but was measured having -0.76 mm. This is most likely due to the difference in coordinate systems and slightly different geometries between the FEA model and the actual wheel used, as mentioned in the expected results section. The predictions were still useful in providing us the correct trends and identifying the areas of highest deflection. As would be expected the highest deflections occurred on the wall of the wheel, which acts similar to a cantilever beam. This information is important for wheel performance because a high compliance wheel may cause suspension geometry to become unpredictable even for relatively small changes.

We found that the max principal strain matched our intuition and FEA model, and was highest at the two edge of our area of focus, near the bolts and on the wheel wall. The average max principal strain value was measured at 4.40E-4, varying from the predicted value of 4.88E-4 by 9.8%. This is helpful in understanding the design of the wheel, and the most likely areas for failure. Looking at the Exx strain, though we find fairly significant differences in average values between the predicted and measured, we again see a similar trend in how the strain forms. For example, the FEA shows a very low positive strain just before the radius upper radius that begins increasing in the negative direction as you travel into the radius and up the wall. This same trend is seen in the DIC data.

While this project generated some useful results and provided a better understanding of the wheel, there are multiple improvements that could be made for future testing. First, due to the very fine speckle size, only a small portion of the wheel could be captured by DIC. Also, expanding the area of interest on our data led to distortions in the plots due to the orientation of each camera with respect to each other. It would have been beneficial to have been able to gather data further up the wall of the wheel as deflection would be significantly higher at these locations. This issue could be solved with a more coarse speckle and a larger viewing window, or multiple camera pairs to capture separate areas of the wheel. Another issue with our test was the loading device which had a circular foot and meant that the device had to be offset from center to avoid contact with the outer lip of the wheel. Also, while the wheel was loaded up to 7000 N, around 5000N the back end of the load device contacted another section of the wheel changing the loading conditions. For future tests, another loading device should be made that would better suit the required loading.



Figure 16.
Loading of wheel on
Instron

References

1. Aluminum 6061-T6; 6061-T651. (n.d.). Retrieved March 23, 2018, from <http://asm.matweb.com/search/SpecificMaterial.asp?bassnum=ma6061t6>